Ion-water coupling controls class A GPCR signal transduction pathways

Neil J. Thomson[1], Owen N. Vickery[1,2], Callum M. Ives[1], and Ulrich Zachariae[1,✉]

[1]Computational Biology, School of Life Sciences, University of Dundee, Dundee DD1 5EH, UK.,
[2]Current address: School of Life Sciences, University of Warwick, Coventry CV4 7AL, UK.,

G-protein-coupled receptors (GPCRs) are membrane proteins that transmit signals across the cell membrane by activating intracellular G-proteins in response to extracellular ligand binding. A large majority of GPCRs are characterised by an evolutionarily conserved activation mechanism, involving the reorientation of helices and the conformation of key residue side chains, rearrangement of an internal hydrogen bonding network, and the expulsion of a sodium ion from a binding site in the transmembrane region. However, how sodium, internal water, and protein residues interplay to determine the overall receptor state remains elusive. Here, we develop and apply "State Specific Information" (SSI), a novel methodology based on information theory, to resolve signal transmission pathways through the proteins. Using all-atom molecular dynamics simulations of pharmaceutically important GPCRs, we find that sodium plays a causal role in the formation and regulation of a communication channel from the ion binding site to the G-protein binding region. Our analysis reveals that the reorientation of specific water molecules is essential to enable coupled conformational state changes of protein residues along this pathway, ultimately modulating the G-protein binding site. Furthermore, we show that protonation of the ion binding site creates a conformational coupling between two previously separate motifs, entirely controlled by the orientation of two water molecules, priming the receptor for activation. Taken together, our results demonstrate that sodium serves as a master switch, acting in conjunction with the network of internal water molecules, to determine the micro- and macrostates of GPCRs during the receptors' transition to activation.

Correspondence: ***u.zachariae@dundee.ac.uk***

Introduction

G-protein coupled receptors (GPCRs) form the largest superfamily of cell surface receptors with over 800 members that control a broad range of physiological processes. GPCRs span the plasma membrane of the cell from the extracellular to the intracellular face and act as signal transducers that enable transmembrane communication between the outside and inside of the cell. Ligand interaction on the extracellular domain induces conformational changes that expose binding sites on the intracellular face, initiating intracellular signalling by binding various effector proteins including heterotrimeric G-proteins and β-arrestins, each of which cause different physiological changes (1). As such, GPCRs form the main target for drug therapies, with over 30% of US food and drug administration (FDA) approved drugs targeting about 108 different GPCRs (2).

With over 700 members, class A receptors comprise the vast majority of GPCRs. High-resolution crystal structures of inactive class A GPCRs have resolved a sodium ion (Na^+) bound to a highly conserved residue central to the transmembrane (TM) domain (residue D2.50 - Ballesteros-Weinstein numbering system). However, this sodium ion is not present in active state crystal structures, implicating the ion in GPCR activation (3–5). In addition, it has been suggested that the presence of a conserved network of internal water molecules connecting polar residues, including D2.50, likely plays an important role in GPCR signal transduction. Through molecular dynamics simulations of a range of class A GPCRs, Venkatakrishnan *et al*. revealed the presence of well-defined water pockets that are conserved across both active and inactive states and further, state-dependent water sites (6). Upon activation, a significant re-positioning of the TM water-network seems to be coupled to the collapse of the sodium binding pocket, though the functional significance of these waters is unknown (6–8).

Various studies have correlated GPCR activation with transitions between distinct rotameric conformations of evolutionarily conserved residues termed microswitches. These rotamer transitions are thought to underpin the large scale conformational changes that govern activation (1, 7, 9–16). Many microswitches form distinct motifs, such as the CWxP motif at the ligand binding site, which is known to link directly to the sodium ion binding pocket (5). The NPxxY motif is also located proximal to the ion binding site and includes Y7.53, which was shown by previous simulation studies to regulate the opening of a transmembrane water channel (8, 17). In addition, the DRY motif at the intracellular face plays a role in G-protein binding, and forms ionic locks that maintain the inactive receptor state (1, 13) (Fig. 1).

These observations suggest that the ion binding site, water mediated interactions, and conserved residues are critical for G-protein signalling. However so far, the functional interaction of these components has remained unknown (5, 6, 18). To resolve their role in enabling receptor movements leading to activation, we designed a new methodology focusing on causation rather than correlation in analysing protein dynamics, which we term "State Specific Information" (SSI).

GPCR signal transduction is a process whereby information is sent, encoded, transmitted and received, in parallel with the tenets of an information system (19). Therefore, sodium, internal water, and microswitches can be seen to act as essential components of an information system. SSI combines Shannon's conditional entropy (19, 20) and McGill's interaction information (also called co-information) (21–24) to quantify how much information, specific to a certain residue or cofactor state, is shared between coupled transitions in residue and cofactor networks. Contrasting traditional correlation approaches that calculate mutual information based on residue covariance (23, 25–27), SSI is closely aligned with

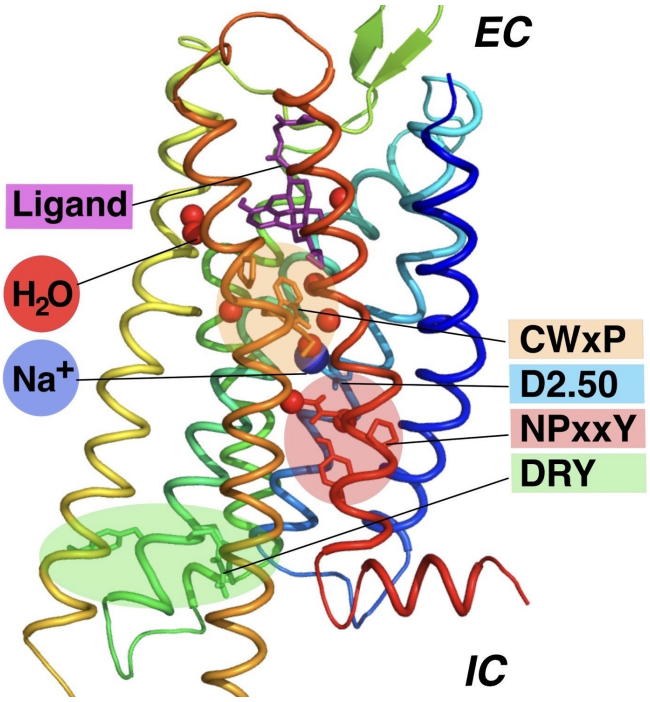

Fig. 1. Class A GPCR key features. The ligand binding pocket, internal waters, sodium ion (Na^+), conserved microswitch motifs, and primary sodium binding residue D2.50 in the μ-opioid receptor (pdb: 4dkl). EC, extracellular and IC, intracellular side.

the concept of microswitches by requiring residues to have at least two conformational states to exchange any information. Thereby, we identify whether a change in the conformational state of one residue is triggered by a conformational state change of another residue, through an inter-dependency between the two residues conformations. This way, we extract information from large-scale, persistent changes between conformational states of these residues.

Our analysis was based on all-atom molecular dynamics simulations that we started from three inactive-state, antagonist-bound class A GPCRs: the A_{2A}-adenosine receptor (A_{2A}AR), the μ-opioid receptor (μOR), and the δ-opioid receptor (δOR). Sodium is believed to reduce the thermal fluctuation level of the protein, thereby stabilising inactive conformations of microswitches (10, 27–29), but the mechanisms by which this is achieved are unknown. Therefore, for each receptor, we collected simulation data on 1.7 μs timescales performed in three different receptor states of the main ion binding residue: D2.50 in a charged state with sodium bound (state Na^+/D^-), D2.50 in a charged state with sodium removed (state $0/D^-$), and D2.50 in a protonated state without sodium (state $0/D^n$). The protonated state of D2.50 was included since earlier observations suggested that the absence of sodium likely triggers D2.50-protonation (17, 27, 30).

Our results show how sodium, protonation, internal water molecules, and the receptor microswitch conformations are coupled to form efficient information transfer pathways from the extracellular to the intracellular side of the receptors. Sodium is found to act as the master switch turning on and off communication with the G-protein binding site.

Results

GPCR-internal water molecules act as microswitches coupled to sodium expulsion and D2.50-protonation. Applying our new approach, "SSI", to microsecond timescale simulations of multiple GPCRs, we identified information pathways specific to the ion binding state of D2.50, and quantified the amount of ion binding information exchanged across networks of coupled residue and water state transitions.

After concatenating trajectories of states Na^+/D^- and $0/D^-$, and states $0/D^-$ and $0/D^n$, SSI was calculated between 7875 residue and internal water pairs. In information theoretic terms, this concatenation represents the binary effect of expelling sodium, and subsequently protonating D2.50 in the receptor. Each process corresponds to 1 bit of information (e.g. 'protonated or de-protonated'), which we term "information source". Focusing on information transferred through residue side chain movements, we investigated the side chain dihedral angles of all Ballesteros-Weinstein positions common to all three receptors from the intracellular face to the base of the orthosteric pocket, including the CWxP motif, totalling 121 residues (Fig. 2A).

Five water pockets that exhibited large probability densities for receptor-internal water molecules in all three receptor simulations (Fig. 2B) were added to the set of residues for SSI investigation by pocket occupancy as well as water orientation (Methods). Four of these water sites were previously identified to be conserved in GPCRs by Venkatakrishnan *et al.* (6).

For sodium expulsion, information specific to the sodium binding state is focused on a small group of important microswitch pairs (5%). Similarly, for D2.50-protonation, SSI is shared between roughly 6% of key microswitch pairs. Notably, our analysis reveals long-range communication between the ion binding site, the NPxxY motif, and the distal DRY motif at the G-protein binding site (Fig. 2C). For example, the conformation of residue R3.50 of the DRY motif, at a distance of ∼22 Å, is strongly affected by D2.50-protonation. In addition, we find that internal water molecules act as key players in transmitting information from the ion binding site. The states of these water molecules are more indicative of the ion binding states of D2.50 than the majority of the protein residues (Fig. 2C). These results suggest that water molecules are an integral part of the signal transmission mechanism. They will henceforth be included in our work as additional elements of an extended set of microswitches.

Ion binding state of D2.50 controls an information pathway to the intracellular DRY motif. The total-SSI of each microswitch quantifies how much information about the state of D2.50 each microswitch exchanges with the receptor overall (see Methods). Fig. 3 displays the 'communication hubs' within the receptor, based on their total-SSI. Sodium expulsion and D2.50-protonation cause unique changes to similar regions of the protein (Fig. 3A). For both information sources, the total-SSI values reveal a pathway that includes water and transmits information from the ion binding site at

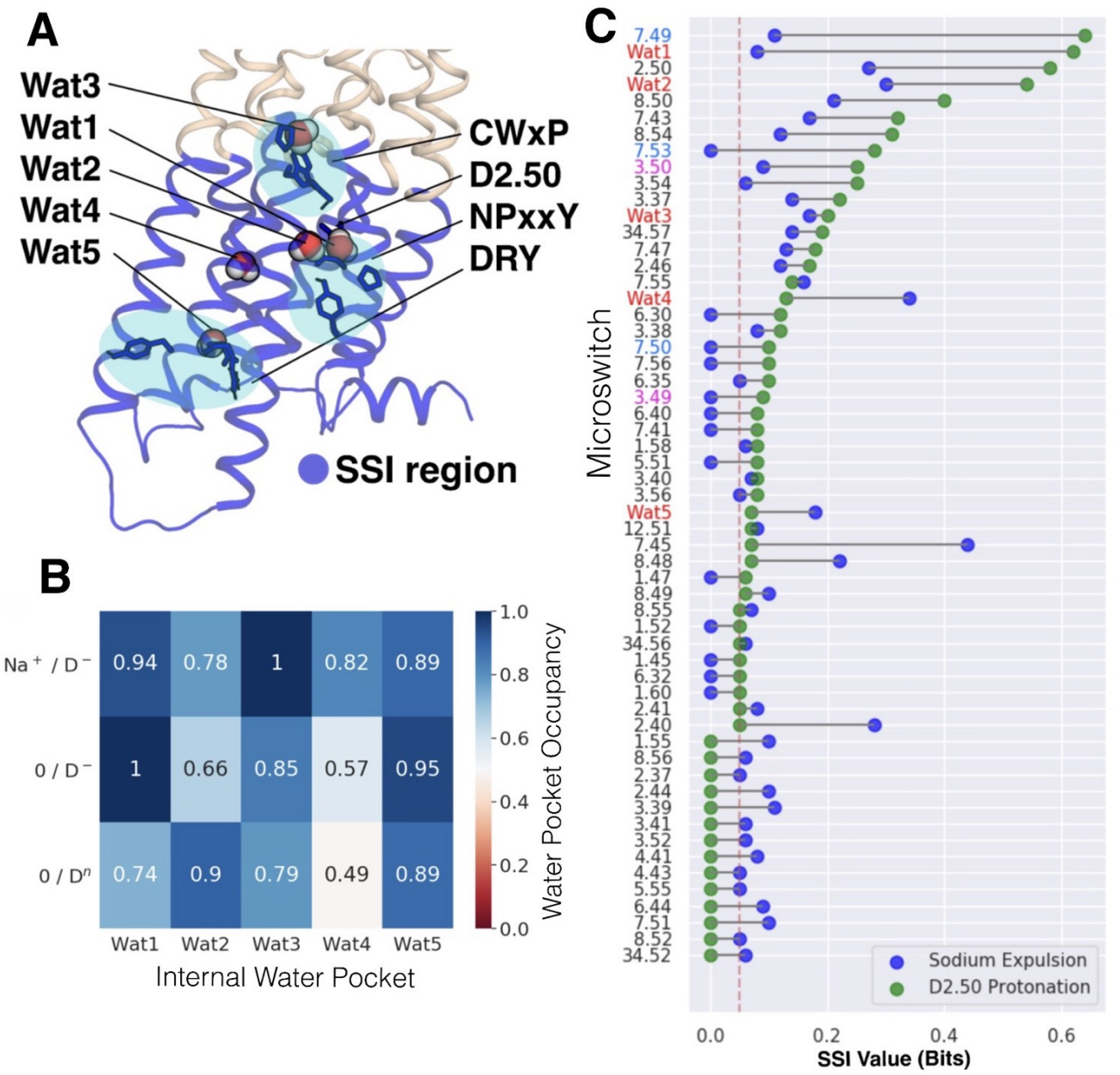

Fig. 2. State Specific Information reveals information flow propagating through the receptor. **(A)** Location of the five water molecules investigated (Wat1–5) with respect to key receptor motifs, and receptor region involved in SSI investigation for μOR (purple region). Wat1 resides beside D2.50, Wat2 beside the NPxxY motif, Wat3 beside the CWxP motif, Wat4 beside W4.50, and Wat5 beside the DRY motif. **(B)** Water pocket occupancy averaged across all three receptors throughout the simulations; a value of 1 reflects complete occupancy in all receptors over the entire simulated time. **(C)** SSI is passed on from the information source to protein microswitches and internal water molecules. Shown are all significant SSI values in bits, shared between both information sources (sodium expulsion and D2.50-protonation: 1 bit each) and each microswitch. High SSI values reflect microswitches that have a highly specific conformational state preference for each of the D2.50 ion binding states. Both information sources uniquely alter the presence and orientation of all five investigated internal water molecules (Wat1-Wat5) as well as having a long-range impact on the conformational state of the DRY motif. The significance threshold is depicted by a vertical red dashed line (0.05 bits), internal water is highlighted in red, residues of the NPxxY motif in blue, and DRY motif residues in magenta.

D2.50, along helix 7 (H7) and across the base of helix 2 (H2) to the distal G-protein binding site at the DRY motif on helix 3 (H3, Fig. 3B). We term this route the H2-7-3 information pathway.

To determine whether the microswitches within this pathway are intricately connected with each other, transferring ion binding information in a 'domino-like' succession of conformational changes of neighbouring microswitches, we used network analysis together with a structural filter for spatially detached SSI pairs (see Methods). Simple pathways of conformational changes bridging between the ion binding site and the G-protein binding site along the H2-7-3 route are detected for both information sources (Figs. 3C, S5). This connectivity forms a causal relationship that allows ion binding changes at D2.50 to affect the conformation of the distal DRY motif.

Ion binding changes at D2.50 trigger concerted conformational changes that funnel SSI from microswitches proximal to the ion binding site further along the H2-7-3 route. Following protonation of D2.50, we also find the conformational change at R3.50 impacts the conformation of residue x6.30 (the helix 6 ionic lock), and position x34.57 on intracellular loop 2 (ICL2) - known to play a significant role in effector protein binding specificity and bias. As SSI and co-SSI are symmetrical quantities, the identified information pathway is equally able to send information from the DRY motif, for example caused by G-protein binding, to the ion binding site.

D2.50-protonation establishes communication between the NPxxY and DRY motifs. Significant SSI is shared between the NPxxY motif and the DRY motif at the G-protein binding site upon D2.50-protonation, but not upon sodium expulsion, showing that these motifs exclusively communicate information specific to the protonation state of D2.50 (for full SSI data see Supplementary Information). Unlike sodium expulsion, D2.50-protonation causes all residues of the NPxxY motif, including P7.50, to undergo various degrees of conformational rearrangement. This highlights that D2.50-protonation promotes inward kinking of helix 7 and alters the conformation of the hydrophobic barrier created by Y7.53 (17) (Fig. 4).

To elucidate the molecular mechanism of information transfer propagating from the ion binding site, we analysed the nature of conformational changes across the receptor. Our simulations show that near the ion binding site, N7.49 bonds its amino group to the side chain oxygen of charged D2.50, irrespective of the presence of sodium. The side chain oxygen of D2.50 also acts as a H-bond acceptor for Wat1, mediating a bond with N1.50 in this state (Fig. 4A). D2.50-protonation triggers substantial rearrangements in its proximity in all three receptor types. The altered H-bonding pattern induces a change to the rotamer state of N7.49, while simultaneously, Wat1 changes dipole orientation (Fig. 4A). The new arrangement is stabilised by a H-bond between the N7.49 side chain oxygen and Wat1.

SSI shows that reorientation of Wat1 affects the conformation of Y7.53, whose OH group points towards the Wat1 pocket in the both deprotonated receptor states, but not the protonated state (Fig. 4A). This is tightly related to the observation that water molecules form a bridge between D2.50 and Y7.53 only when sodium is bound. Y7.53 flips into its downward state (previously correlated with opening a hydrophobic gate (8, 17)) in the protonated A_{2A}AR and μOR, and in the δOR upon further protonation of D3.49. The protonation-dependent downward movement of Y7.53 in the μOR and A_{2A}AR then ultimately triggers an upward swing of R3.50 into its active, G-protein binding conformation, as demonstrated by the SSI shared between these microswitches.

In addition, the inter-hydroxyl distance between Y7.53 and Y5.58 is reduced. In the μOR, D2.50-protonation is sufficient to decrease the Y7.53-Y5.58 inter-hydroxyl distance to the distribution seen in the active state, as compared to data from a 1.7-μs simulation of the active crystal structure (pdb: 6ddf) (Fig. S3). We also find that the G-protein binding cavity opens upon further protonation of D3.49 in the δOR, as measured by the TM2-TM6 activation coordinate between T2.39-Cα and I6.33-Cα (Fig. S4). Furthermore, in the D2.50-protonated receptor, N1.50 and P34.50 occupy well-defined, singular conformations. This demonstrates that protonation stabilises a specific conformational state of ICL2 at the G-protein binding interface.

Polar networks proximal to the ion binding site govern microswitch conformations via GPCR-internal water molecules. To study the functional role of the internal water network in more detail, we employed interaction or co-information (co-SSI) (21–23). Co-SSI quantifies the effect of intercalated water molecules Wat1-Wat5 on information transfer between pairs of microswitches. Positive co-SSI indicates that microswitch conformations, specific to the ion binding state of D2.50, are stabilised by their interaction with water molecules, amplifying their shared information. There are different interpretations of negative co-information values in the literature (22–24). Here, in accordance with the results from LeVine & Weinstein (23), we interpret negative co-information as destabilisation of state specific microswitch conformations by their interaction with water molecules, attenuating their shared information.

As shown by co-SSI, the water network has a particularly pronounced effect on the H2-7-3 pathway upon D2.50-protonation (Fig. 4C,D). Specifically, co-SSI values demonstrate that the D2.50-protonated conformations of Wat1 and Wat2 significantly stabilise the conformational reorientation along the H2-7-3 channel. This indicates that reorientation of Wat1 and Wat2 is critical to enable the transmission of information about D2.50-protonation throughout the receptor, and establish communication between the NPxxY and DRY motifs. The negative value of co-SSI between P7.50, Wat1, and the information source, by contrast, implies that Wat1 destabilises the conformational state of P7.50 upon D2.50-protonation, contributing to the kinking of helix 7.

The SSI values show that the three D2.50 ion binding states (Na^+/D^-, 0/D^-, and 0/D^n) all induce unique configurations of five microswitches located in the D2.50-proximal polar network – D2.50, N7.45, N7.49, Wat1, and Wat2. High total-SSI and co-SSI values suggest that a fine tuning of the

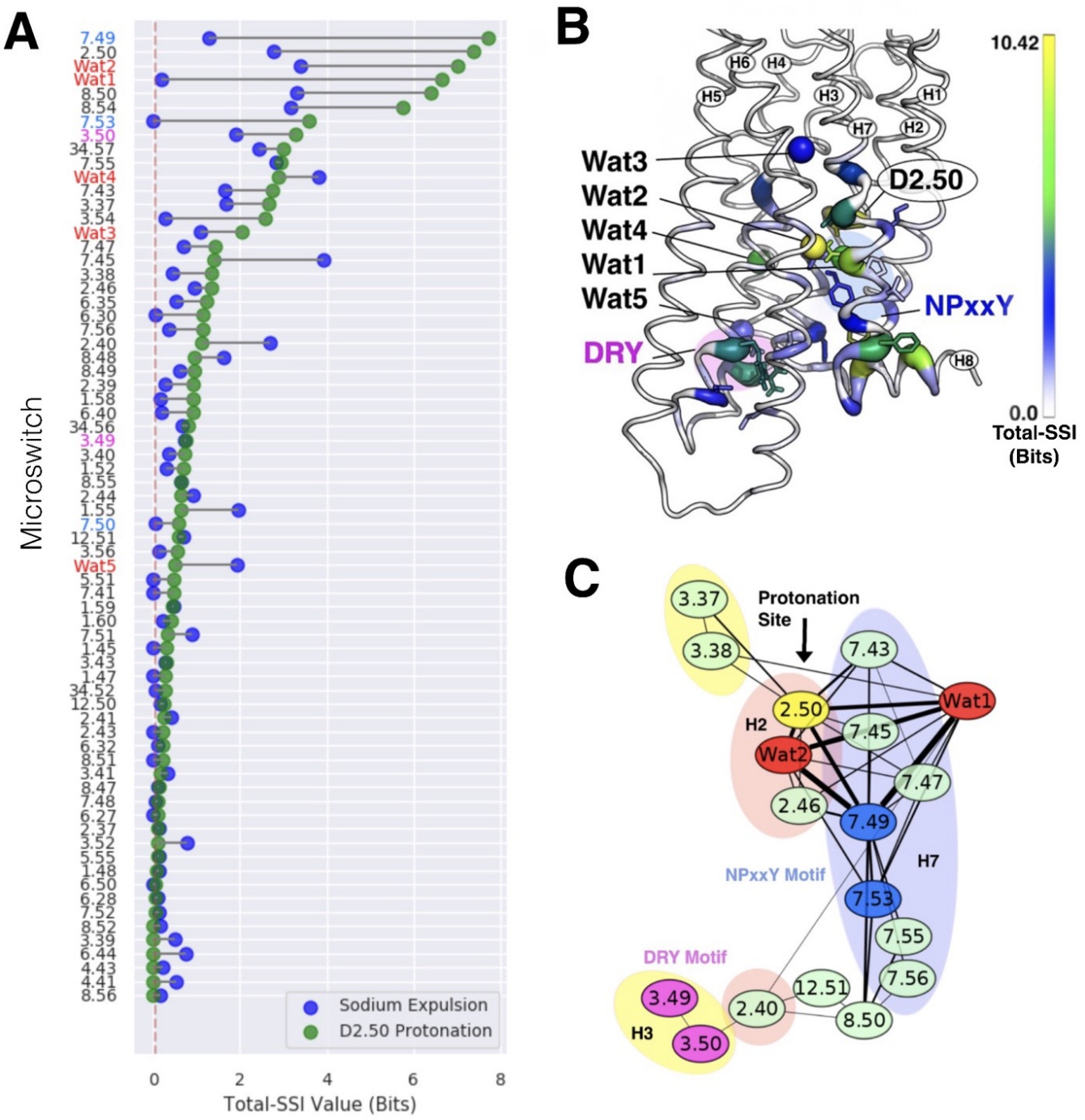

Fig. 3. Communication hubs in class A GPCRs form a pathway between the ion binding site and G-protein binding site. (A) All non-zero total-SSI values for each microswitch, quantifying each microswitches communication with the rest of the receptor. Internal water is highlighted in red, residues of the NPxxY motif in blue, and DRY motif residues in magenta. **(B)** Total-SSI values (bits), summed across both information sources sodium expulsion and D2.50-protonation, projected as colour-code (from white, 0 bits to yellow, 10.42 bits) onto the μOR crystal structure (pdb:4dkl). Key microswitches are shown as sticks, water molecules as spheres. The information hotspots bridge the ion binding site and the DRY motif at the G-protein binding site. Information about the ion binding state of D2.50 is transmitted on this pathway to the intracellular face. **(C)** Pathways bridging between D2.50 (ion binding site) and the DRY motif (G-protein binding region) transfer D2.50-protonation information through spatially neighbouring microswitches. Microswitches are represented by nodes labelled with their corresponding Ballesteros-Weinstein numbers. Edges between nodes represent information transfer; the edge width is proportional to the magnitude of shared SSI.

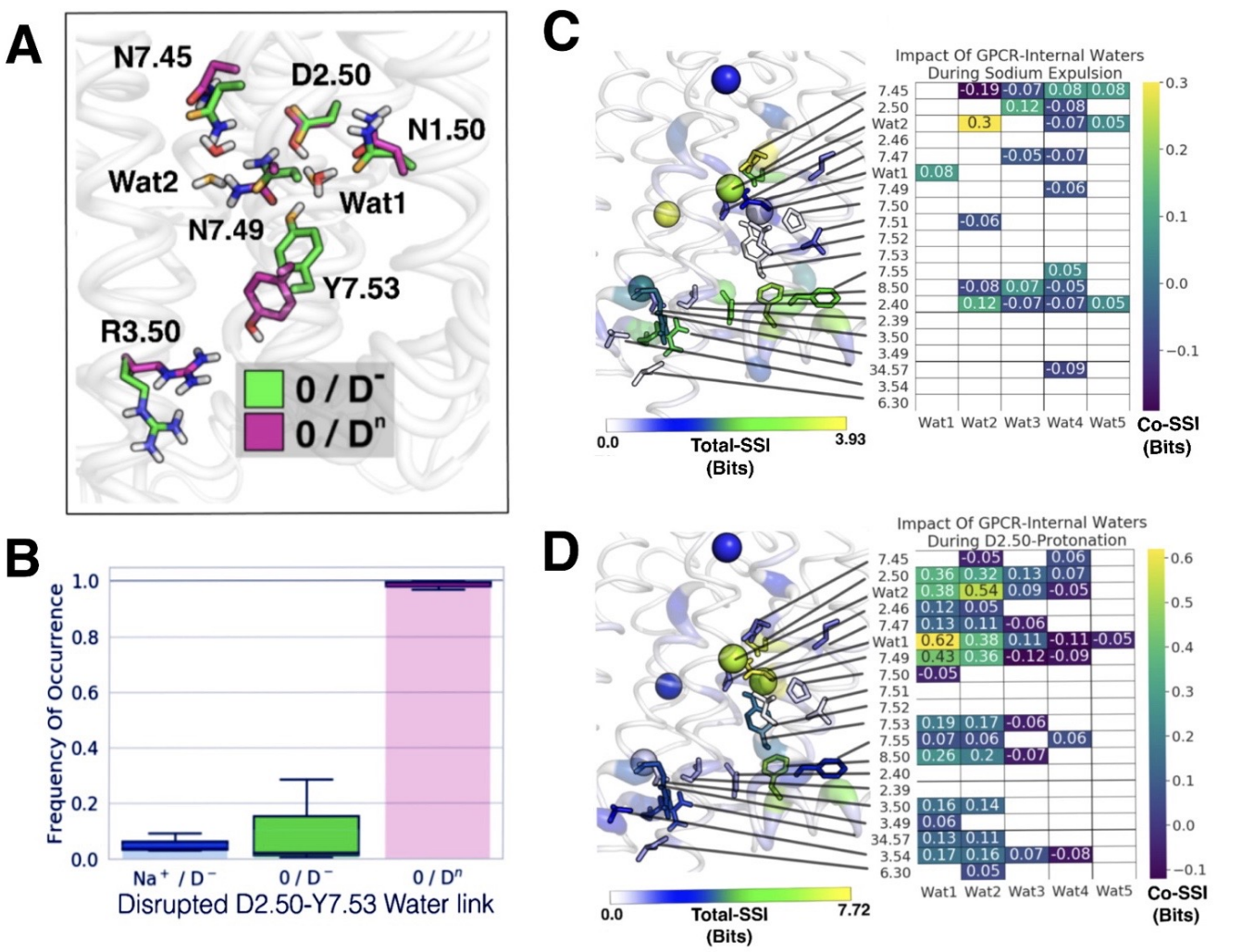

Fig. 4. Protonation establishes communication between NPxxY motif and DRY motif by rotating water molecules. Exemplar frames from molecular dynamics simulations of μOR in states 0/D$^-$ and 0/D^n **(A)** and normalised count of water bridge formation between D2.50 and Y7.53 in all three D2.50 states, averaged across the three receptors **(B)**. For state 0/D$^-$, side chain carbon atoms are coloured in green and oxygen atoms (side chain and water) are coloured in orange. In state 0/D^n, carbon atoms are shown in magenta and oxygen atoms in red. The bridge locks Y7.53 in an upward-oriented state. D2.50-protonation results in a rotation of water molecule Wat1 and the side chain conformation of N7.49, leading to breakage of the water bridge. Y7.53 then flips downwards, and R3.50 moves upwards in concerted fashion, forming a water-mediated bond between the DRY and NPxxY motif. **(C, D)** Impact of the five water molecules on SSI transfer along the H2-7-3 channel arising from the information sources sodium expulsion **(C)** and D2.50-protonation **(D)**, with total-SSI heatplots for only D2.50-protonation projected onto the μOR structure on the left (pdb: 4dkl). Positive co-information values characterise water molecules (table columns) that amplify shared information between any specific microswitch (table rows) and the information source, whereas negative values reflect attenuation of information transmission. Protonation of D2.50 unlocks water states allowing them to amplify signal transfer along the channel. When two of the three co-SSI components are the same, co-SSI equals the SSI between the two differing components.

conformational states of these residues ultimately determines the conformational rearrangement at the distal DRY motif. We find that the ions tune the conformational states in the D2.50-proximal polar network through alterations to the local hydrogen bonding patterns (Fig. 5A). In turn, these configurations funnel information about the ion binding state of D2.50 into the H2-7-3 pathway, as can be seen in Fig. 3. Our results thus suggest that the proximal polar network around D2.50, formed by water molecules and conserved polar residues, governs long-distance communication through class A GPCRs, and that the local network itself is controlled by binding and release of sodium and D2.50-protonation.

Sodium restrains key microswitches to a single conformation. The sodium-bound form of class A GPCRs is associated with their inactive state (4, 5, 17, 31). Our simulations with bound sodium (Na^+/D^-) display decreased disorder in the conformations of D2.50, N7.45, P7.50, x7.51, Y7.53, F8.50, N2.40, R3.50, and x6.30, the majority of which feature in the H2-7-3 pathway (Fig. 5B). The conformational state entropy (see Methods) of the sodium-bound conformations of D2.50 and Y7.53 is decreased to zero in all three receptors, which means that these residues occupy one highly ordered, well-defined conformation throughout the trajectories. Notably, two further microswitches show zero entropy, i.e. confinement to a single conformation, for the sodium-bound state, N1.50 (a 100% conserved residue) and P5.50 (P-I-F motif).

The coupling between well-defined, singular conformational states of D2.50, N1.50 and Y7.53 correlates with our observation that a water wire exists between these microswitches in the sodium-bound state, and explains the absence of infor-

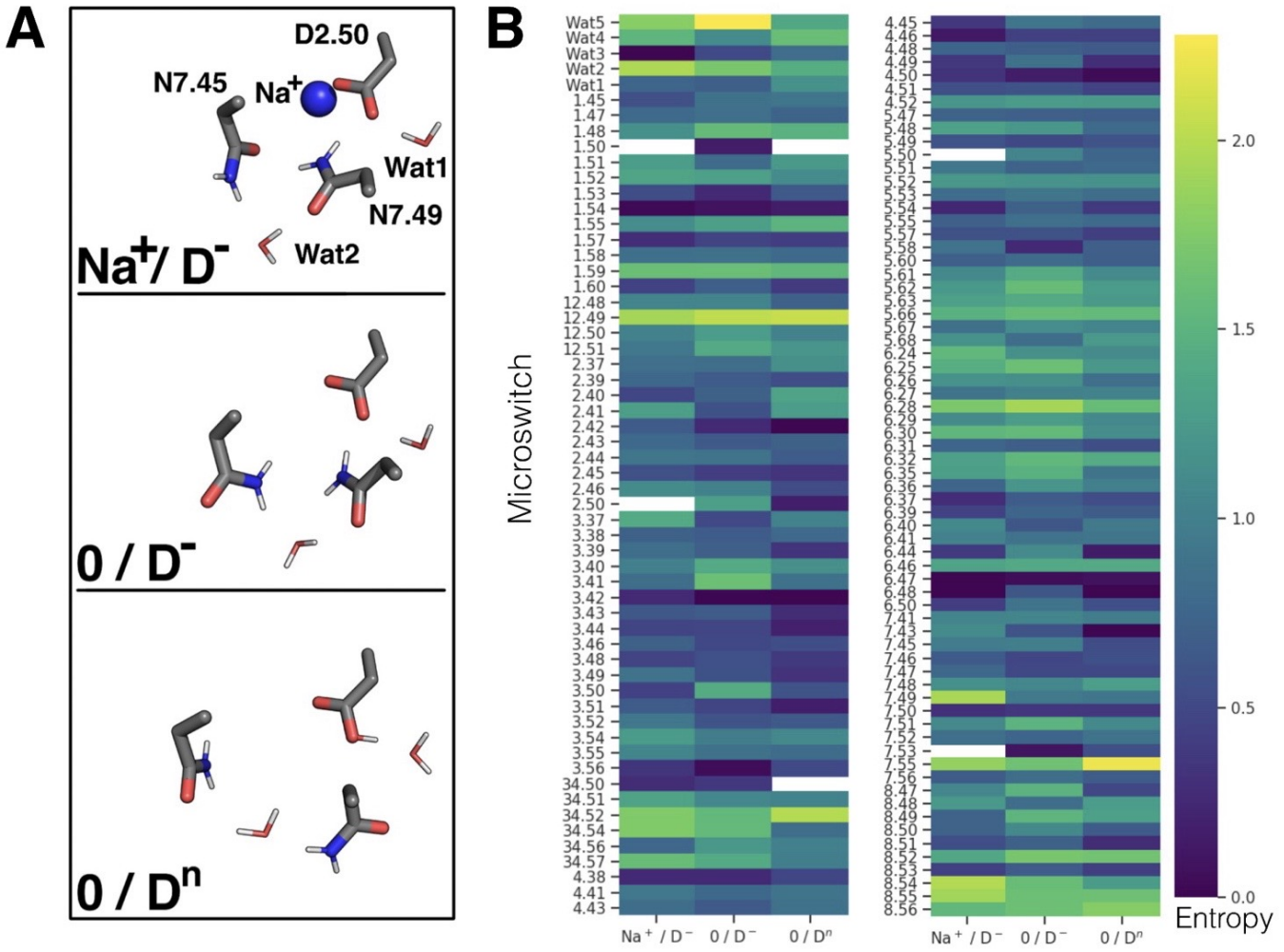

Fig. 5. Unique configurations of the D2.50-proximal polar network depending on sodium presence. Schematic illustration of the D2.50-proximal polar network tuning downstream conformational states in the information channel **A**. In this schematic red and blue depict positive and negative poles (partial charges), respectively. Sodium expulsion alters the hydrogen bonding pattern between D2.50 and N7.45 by rotating the side chain conformation of N7.45. D2.50-Protonation alters the hydrogen bonding pattern between D2.50 and N7.49 by rotating the side chain conformation of N7.49. The two conformations of N7.45 and N7.49 are stabilised by water molecules Wat1 and Wat2. Microswitch entropies for all three D2.50-state simulations, averaged across the A_{2A}-adenosine, δ-opioid, and μ-opioid receptors **B**. White rectangles represent microswitches with zero entropy, i.e. occupying one singular conformation throughout the entire trajectory for all three receptors. Entropies greater than zero are represented by the heatmap ranging from blue (minimum non-zero entropy) to yellow (maximum entropy).

mation shared between Y7.53 and the DRY motif. By contrast, in addition to observing microswitch conformational state fluctuations in the sodium-free (0/D$^-$) simulations, all microswitches display some magnitude of state entropy. In the protonated D2.50 state, only N1.50 is restrained to a single conformation in its vicinity. In summary, we conclude that sodium holds the receptor in the inactive state by restraining the key microswitches D2.50, Y7.53, N1.50, and P5.50 to single conformations, which are unable to participate in information transfer, disconnecting the information transfer route across the receptors.

Discussion

It has been recognised previously that internal water molecules (6, 10) and a sodium ion bound to a highly conserved binding site (4, 17, 31) likely play a key part in activating class A GPCRs. However, the functional role of these cofactors and their interaction with the protein had been poorly understood. Similarly, conformational changes of key conserved residues in the receptors – microswitches – have been known to be associated with activation (1, 9). However, how the transitions of individual microswitches act in concert with each other to transmit signals across the entire protein, and how these changes are interconnected with the water and ion network had remained unclear.

In the present work we have joined the various strands of knowledge together and reveal by a new methodology that sodium acts as the master switch for regulating a long-range information transfer pathway across the receptor. This pathway carries information about the ion binding state of D2.50 from the extracellular binding pocket to the DRY motif at the intracellular G-protein binding site along receptor helices 2, 7, and 3 (H2-7-3 pathway). Information is exchanged along this pathway especially upon protonation of the ion binding residue D2.50, which is controlled by the presence of sodium (17, 30). Furthermore, we find that the ability to transfer in-

formation along this pathway crucially depends on the function of the water molecules that occupy conserved protein cavity sites between key protein microswitches, whose orientations are coupled to changes at the ion binding site. This suggests that these water molecules act as an extended set of microswitches.

Since transmembrane signal transduction is a process of information transfer, we developed a new methodology based on the principles of Shannon's information theory and co-information (19, 21). Our methodology, termed "State Specific Information" (SSI), traces information pathways through coupled transitions in residue and cofactor conformational state changes, such as those between active and inactive receptor microswitches, which are caused by receiving a signal on one side of the GPCR (15, 16). SSI is however not limited to GPCRs. It is applicable to identify and quantify pathways of information flow caused by any trigger, such as binding of a ligand or protein, that are encoded in any conformational state changes of protein components. This methodology differs from traditional approaches that focus on correlated residue or atom fluctuations (23, 25, 26, 32) by requiring significant and persistent conformational state changes that are coupled to a specific cause. The incorporation of causality is further emphasised by the use of co-SSI (24).

A sodium ion bound to D2.50 is linked to the inactive state of GPCRs, as shown by a range of inactive crystal structures (5). In our simulations, the presence of sodium induces a unique conformation of the polar network that surrounds the ion binding site at D2.50. Coupled to the existence of a water wire between D2.50 and Y7.53, the sodium-bound configuration tightly restrains Y7.53 to its inactive conformation, oriented towards N7.49. Thereby, sodium binding disconnects the information transfer route between the NPxxY motif and the DRY motif. In contrast, the sodium-free, D2.50-charged ($0/D^{-}$) configuration of the D2.50-proximal polar network is unstable, enabling all microswitches to sample more than one conformation, and triggering a series of conformational changes that propagate ion binding information via the H2-7-3 pathway.

Similarly, D2.50-protonation induces a unique configuration of the D2.50-proximal polar network, rotating water 1 (see Fig. 4) and eliminating the water bridge between Y7.53 and D2.50, which releases Y7.53 from its inactive conformation. This change establishes long distance information transfer, specific to the D2.50-protonation state, between the NPxxY motif and DRY motif. We conclude that sodium expulsion releases a tight restraint on the conformation of key microswitches, in contrast to D2.50-protonation, which causes microswitches to adopt more distinct conformational states. In both steps, reorientation of the internal water molecules in GPCRs play an essential part.

Even in the presence of a bound antagonist, we observe conformational rearrangements for highly conserved microswitches in the DRY and NPxxY motif of three receptors upon protonation, which mimic those observed in the transition between inactive and active state crystal structures. This is in line with prior reports, in which absence of the sodium ion and protonation had been suggested to trigger long-lived active states of the receptors (17) as well as the observation that active state structures exhibit no bound sodium (5).

Only a small fraction of class A GPCRs do not possess a sodium binding site in their transmembrane domain (for example the NK1 neurokinin receptor (5, 33)), however they contain a similarly dense internal network of polar residues and water. A sodium-independent mechanism of controlling protonation and reorientation of this polar network is conceivable in these receptors. However, future studies will be necessary to confirm if the polar signal transmission and activation mechanism we find is conserved in the limited number of atypical class A GPCRs.

Methods.

Information Theory. The current consensus in the field is that slow modes in protein dynamics, for instance those of GPCR microswitches, have the greatest functional relevance, as they represent large scale changes between conformational states, rather than high frequency oscillations of the same conformational state (34). Therefore, in order to obtain mutual information between low frequency changes to microswitch rotamers, our methodology, state-specific information (SSI), differs from traditional approaches to derive mutual information from atom or residue covariance during MD simulations (23, 25, 26, 32). In SSI, residue side chains are required to have at least two conformational states to store any information, e.g. 'up' and 'down' in the simplest case. By looking at the state of one residue, we can infer about the state of another, forming the first element of an information pathway. Deriving mutual information from long-lived conformational states rather than residue fluctuations eliminates noise from co-varying residues that always occupy the same conformation, while highlighting residues that are conformationally linked.

The analysis was divided into three pairwise combinations of the three ion binding states of D2.50, isolating the functional effect of removing sodium from that of protonating D2.50. In this way, we focused on residue (and water) configurational changes that can be traced back to a certain cause, as opposed to pure correlative measures. The pairwise combinations of simulations were concatenated to create one larger trajectory representing the change in state of D2.50: removal of sodium (sodium-bound D2.50 [Na^{+}/D^{-}] + charged D2.50 [$0/D^{-}$]), and protonation of D2.50 (charged D2.50 [$0/D^{-}$] + protonated D2.50 [$0/D^{n}$]). Protonation was previously hypothesised to occur at the ion binding site during sodium removal and activation (17). The 'source information', which corresponds to the cause of the associated conformational changes, depends on the pairwise combination of simulations used, and represents the binary change made to the state of the ion binding site (i.e., 1 bit of information – sodium-bound to sodium-free; and sodium-bound or -free to protonated). All values of mutual and co-information are therefore normalised to 1 bit.

We investigated all residues from the intracellular face to the

base of the orthosteric pocket, including the CWxP motif (Fig. 2A). To focus on information pathways shared between all three receptors, residues whose Ballesteros-Weinstein positions were not common to all three receptors were omitted (for example in loops with differing lengths). Furthermore, we excluded Ballesteros-Weinstein positions that did not have variable side chain dihedral angles in all three receptors, resulting in a total of 121 investigated side chains. We then took the geometric mean of our results across all common Ballesteros-Weinstein positions. Residues whose configurations are dependent on the state of D2.50 respond with distinct changes in their rotamer states. Additionally, by investigating the water occupancy and dynamics of a number of water sites conserved in both inactive and active state crystal structures, we quantified the influence of water on these communication pathways using co-information (also termed interaction information (23)), applied to residue states as co-SSI.

Residue side chain rotamer conformations are defined by in-house Gaussian style clustering to $\chi 1$ and $\chi 2$ dihedral angles, as seen in Fig. 6. A Hanning window function was used to smooth the probability density function to remove noise and locate the state maxima for each rotamer conformation. Guess parameters for Gaussian fitting were then obtained by locating the full-width at half-maximum from each maximum and Gaussian curve fitting was applied. Each discretised distribution was additionally checked visually to ensure the fitting was accurate.

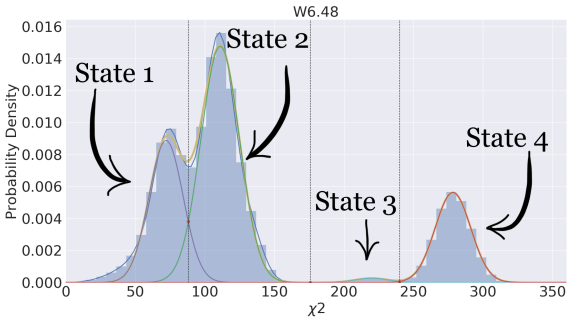

Fig. 6. Illustration of our Gaussian clustering method for defining discrete residue rotamer states. The example given is for the $\chi 2$ angle of the highly conserved tryptophan residue W6.48.

The dipole moment vector of water molecules (μ) was calculated by $\mu = 0.5(H_1 + H_2) - O$, where H_i is the (x,y,z) coordinate of the ith hydrogen, and O is the (x,y,z) coordinate of the oxygen. The orientation of water polarisation was calculated by converting the dot product of the dipole vector with the simulation box axes vectors into spherical coordinates, $\psi = arctan(y/x)$, followed by the same Gaussian style clustering algorithm.

When water is not found in a specific water pocket at a certain time point, that pocket is assigned an empty state. Water pockets must have all three water atoms within the pocket as defined above to be considered occupied. Together, this allowed us to deduce the functional effect of each water pocket on the communication between microswitch pairs.

The conformational state entropy is determined from $H = -\sum_i p(i) log_2 p(i)$, where $p(i)$ is the probability of state i occurring, and H is the entropy, which is also a measure of the maximum information a microswitch can store. A regular average was taken across all common Ballesteros-Weinstein positions in the three receptors to deduce the average entropy of a specific residue.

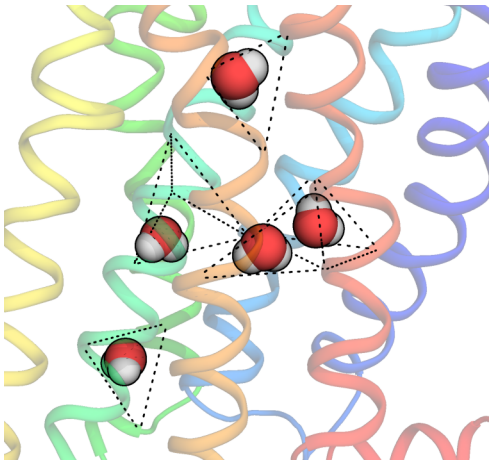

Fig. 7. Water pockets conserved in active and inactive crystal structures of μOR, A_{2A}AR and δOR. Pockets are defined as spheres of radii 4 Å and 5 Å centred on the centre of geometry of the respective triangles and tetrahedrons.

State Specific Information (SSI) between conformational states of two residues X and Y is calculated using $SSI(X,Y) = H(X) + H(Y) - H(X,Y)$, where $H(X|Y)$ is the conditional entropy (19), quantifying here how much the rotameric state of residue X depends on the rotameric state of residue Y. The total-SSI value is obtained from a summation of all SSI values for a particular residue.

The co-information (or interaction information), co-SSI, is calculated using

$$\begin{aligned} coSSI(X,Y,H_2O) &= SSI(X,Y) - SSI(X,Y|H_2O) \\ &= H(X) + H(Y) + H(H_2O) \\ &\quad - H(X,Y) - H(X,H_20) - H(Y,H_2O) \\ &\quad + H(X,Y,H_2O) \end{aligned}$$

where $SSI(X,Y|H_2O)$ determines which magnitude of mutual information shared between X and Y is dependent on the state of a specific third component, often an intercalating water molecule (H_2O) (21). We deem SSI and co-SSI values of less than 0.05 bits insignificant on a 95% significance level.

Network Analysis. To highlight communication between spatially neighbouring microswitches, we filtered the total SSI network based on microswitch SSI values, total-SSI values, and crystal structure positions. To extract information pathways unique to the information source, any microswitch that did not share SSI with the information source was disregarded from the network. Furthermore, only microswitches connected by edges representing SSI $\geq$ 0.06 bits were selected for the network, eliminating pathways of minimal significance (0.05 bits), and a total-SSI threshold of at least 0.149 bits was applied. Additionally, a maximum cutoff distance between the Cα's (ΔCα) of each microswitch pair was

chosen as a proximity criterion. For water molecules, the geometric centre of the water pocket was used instead. Structural analysis was performed on the crystal structure of the A_{2A}-adenosine receptor (A_{2A}AR, pdb:5olz), the μ-opioid receptor (μOR, pdb:4dkl), and the δ-opioid receptor (δOR, pdb:4n6h). SSI values were accepted if the microswitch pairs were within $\Delta C\alpha < 12.3$Å in all three receptors; this threshold is derived from the $\Delta C\alpha$ distance of R3.50 and N2.40 in the δ-opioid crystal structure.

Network analysis was performed using the networkx library in Python (35). For Fig. 3C, we selected all simple pathways bridging between D2.50 and D3.49 with a maximum of 6 interconnecting microswitches (see Supplementary Information for networks including all simple pathways). In a *simple pathway* there are no repeated nodes when forming a pathway between a source node and a target node, i.e. the nodes propagate information from one to another in sequential order.

Protein structure preparations. All crystal structures (μOR - pdb:4dkl, δOR - pdb:4n6h, A_{2A}AR - pdb:5olz) were obtained from GPCRdb (36), selecting the GPCRdb refined structure in which mutations are reversed to the canonical sequence and cleaved loops are re-modelled using MODELLER 9.18 to produce the final structure (37, 38). All transmembrane crystalline waters and ligands were kept in the structure, removing all external waters and non-protein molecules. The proteins were truncated and capped with acetyl and methyl groups at corresponding N and C terminals using PyMOL (39). As the μOR crystal structure did not resolve a sodium ion in the pocket, the sodium-bound structure was obtained by aligning the δOR crystal structure and placing the sodium ion in an identical position. D2.50-charged protein structures were prepared by removing sodium from the crystal structure and ensuring no sodium ion re-associated during the course of the simulation. The third, protonated-D2.50 protein state was prepared in the molecular dynamics software GROMACS-5.1.1 (40). Ligand structures were taken from their respective protein pdb files, and parameterised for molecular dynamics simulations in GROMACS-5.1.1 using ACPYPE (41).

MD simulations. We modelled the protein, membrane, and ligand using the amber99sb-ildn forcefield (42) in GROMACS-5.1.1 with virtual sites to allow a time-step of 4 fs. The proteins were embedded in a pre-equilibrated SLipid POPC membrane (43) using InflateGRO (44). The protein-membrane complexes were solvated with a solution of TIP3P water molecules (45) containing NaCl at 150 mM concentration, with a box size of $\sim$128x134x125 Å^3. The systems were equilibrated in both the NVT and NPT ensembles at 310 K for 3 ns, with a further 70 ns of production run simulation considered as additional NPT equilibration. Following equilibration, simulations were performed for 1.7 μs each at a constant temperature of 310 K and pressure of 1 bar, with the protein-ligand complex, membrane, and solution independently coupled to a temperature bath using a Nosé-Hoover thermostat with a time constant of 0.5 ps and a semi-isotropic Parrinello-Rahman barostat with a time constant of 5 ps (46). The trajectory of the δOR protonated at D2.50 was obtained from a previous simulation study (47, 48). All protein and lipid bond lengths were constrained with the LINCS algorithm (49), while water bond lengths were constrained using SETTLE (50).

Obtaining rotamer angles. Rotamer angles were determined every 120 ps using gmx_chi. The frame separation was chosen to be slightly smaller than the autocorrelation time of the conserved water dynamics with the fastest relaxation time (51). For μOR, water pockets were defined using MDAnalysis (52) as spheres of radius 4 Å centred on the geometric centres of (i) the tetrahedron formed by joining the C-α atoms of N1.50-D2.50-N7.49-L2.46; (ii) the triangle formed by joining the C-α atoms of N7.45-N7.49-A6.38; (iii) the triangle formed by joining the C-α atoms of C6.47-P6.50-C7.37; and (iv,v) spheres of 5 Å radius centred on the geometric centres of the tetrahedron formed by joining the C-α atoms of N2.45-T3.42-V4.45-W4.50, and the triangle V3.48-R34.57-A4.42, respectively. Similar positions were used for the δOR and A_{2A}AR, determined by centering the water probability density in the geometric centre of the selected C-α atoms.

ACKNOWLEDGEMENTS

We thank Seva Katritch for critical reading of the manuscript. This work was supported by a BBSRC EASTBIO PhD studentship (to N.J.T.); a BBSRC Case award (to O.N.V.); and an MRC 4-year PhD studentship (to C.M.I.).

Bibliography

1. Vsevolod Katritch, Vadim Cherezov, and Raymond C Stevens. Structure-Function of the G Protein–Coupled Receptor Superfamily. *Annual Review of Pharmacology and Toxicology*, 53(1):531–556, 2013. doi: 10.1146/annurev-pharmtox-032112-135923.
2. Alexander S Hauser, Sreenivas Chavali, Ikuo Masuho, Leonie J Jahn, Kirill A Martemyanov, David E Gloriam, and M Madan Babu. Pharmacogenomics of GPCR Drug Targets. *Cell*, 172(1):41 – 54.e19, 2018. ISSN 0092-8674. doi: https://doi.org/10.1016/j.cell.2017.11.033.
3. Vignir Isberg, Chris de Graaf, Andrea Bortolato, Vadim Cherezov, Vsevolod Katritch, Fiona H Marshall, Stefan Mordalski, Jean-Philippe Pin, Raymond C Stevens, Gerrit Vriend, and David E Gloriam. Generic GPCR residue numbers – aligning topology maps while minding the gaps. *Trends in Pharmacological Sciences*, 36(1):22–31, 2015. ISSN 0165-6147. doi: https://doi.org/10.1016/j.tips.2014.11.001.
4. Libin Ye, Chris Neale, Adnan Sljoka, Brent Lyda, Dmitry Pichugin, Nobuyuki Tsuchimura, Sacha T Larda, Régis Pomès, Angel E García, Oliver P Ernst, et al. Mechanistic insights into allosteric regulation of the a 2a adenosine g protein-coupled receptor by physiological cations. *Nature communications*, 9(1):1–13, 2018.
5. Barbara Zarzycka, Saheem A. Zaidi, Bryan L. Roth, and Vsevolod Katritch. Harnessing ion-binding sites for GPCR pharmacology. *Pharmacological Reviews*, 71(4):571–595, 2019. ISSN 15210081. doi: 10.1124/pr.119.017863.
6. A J Venkatakrishnan, Anthony K Ma, Rasmus Fonseca, Naomi R Latorraca, Brendan Kelly, Robin M Betz, Chaitanya Asawa, Brian K Kobilka, and Ron O Dror. Diverse GPCRs exhibit conserved water networks for stabilization and activation. *Proceedings of the National Academy of Sciences*, 116(8):3288–3293, 2019. ISSN 0027-8424. doi: 10.1073/pnas.1809251116.
7. A. J. Venkatakrishnan, Xavier Deupi, Guillaume Lebon, Franziska M. Heydenreich, Tilman Flock, Tamara Miljus, Santhanam Balaji, Michel Bouvier, Dmitry B. Veprintsev, Christopher G. Tate, Gebhard F.X. Schertler, and M. Madan Babu. Diverse activation pathways in class A GPCRs converge near the G-protein-coupling region. *Nature*, 536:484–487, 2016. doi: 10.1038/nature19107.
8. Shuguang Yuan, Slawomir Filipek, Krzysztof Palczewski, and Horst Vogel. Activation of G-protein-coupled receptors correlates with the formation of a continuous internal water pathway. *Nature Communications*, 5(4733), 2014. ISSN 20411723. doi: 10.1038/ncomms5733.
9. Vsevolod V Gurevich and Eugenia V Gurevich. Molecular Mechanisms of GPCR Signaling: A Structural Perspective. *International journal of molecular sciences*, 18(12), nov 2017. ISSN 1422-0067. doi: 10.3390/ijms18122519.
10. Leonardo Pardo, Xavier Deupi, Nicole Dölker, María Luz López-Rodríguez, and Mercedes Campillo. The Role of Internal Water Molecules in the Structure and Function of the Rhodopsin Family of G Protein-Coupled Receptors. *ChemBioChem*, 8(1):19–24, jan 2007. ISSN 1439-4227. doi: 10.1002/cbic.200600429.

11. Yoonji Lee, Sun Choi, and Changbong Hyeon. Mapping the intramolecular signal transduction of G-protein coupled receptors. *Proteins: Structure, Function and Bioinformatics*, 82 (5):727–743, 2014. ISSN 10970134. doi: 10.1002/prot.24451.
12. Yoonji Lee, Sun Choi, and Changbong Hyeon. Communication over the Network of Binary Switches Regulates the Activation of A2A Adenosine Receptor. *PLoS Computational Biology*, 11(2):1–21, 2015. ISSN 15537358. doi: 10.1371/journal.pcbi.1004044.
13. B Trzaskowski, D Latek, S Yuan, U Ghoshdastider, A Debinski, and S Filipek. Action of molecular switches in GPCRs–theoretical and experimental studies. *Current medicinal chemistry*, 19(8):1090–1109, 2012. ISSN 1875-533X. doi: 10.2174/092986712799320556.
14. Katsufumi Tomobe, Eiji Yamamoto, Kholmirzo Kholmurodov, and Kenji Yasuoka. Water permeation through the internal water pathway in activated GPCR rhodopsin. *PLoS ONE*, 12(5):e0176876, 2017. ISSN 19326203. doi: 10.1371/journal.pone.0176876.
15. Qingtong Zhou, Dehua Yang, Meng Wu, Yu Guo, Wanjing Guo, Li Zhong, Xiaoqing Cai, Antao Dai, Wonjo Jang, Eugene Shakhnovich, Zhi Jie Liu, Raymond C. Stevens, Nevin A. Lambert, M. Madan Babu, Ming Wei Wang, and Suwen Zhao. Common activation mechanism of class a GPCRs. *eLife*, 8(e50279), 2019. ISSN 2050084X. doi: 10.7554/eLife.50279.
16. Oliver Fleetwood, Pierre Matricon, Jens Carlsson, and Lucie Delemotte. Energy landscapes reveal agonist control of g protein-coupled receptor activation via microswitches. *Biochemistry*, 59(7):880–891, 2020.
17. Owen N Vickery, Catarina A Carvalheda, Saheem A Zaidi, Andrei V Pisliakov, Vsevolod Katritch, and Ulrich Zachariae. Intracellular Transfer of Na+ in an Active-State G-Protein-Coupled Receptor. *Structure*, 26(1):171 – 180.e2, 2018. ISSN 0969-2126. doi: https://doi.org/10.1016/j.str.2017.11.013.
18. I. Rodriguez-Espigares, M. Torrens-Fontanals, J.K.S. Tiemann, et al. Gpcrmd uncovers the dynamics of the 3d-gpcrome. *Nature Methods*, 2020. doi: 10.1038/s41592-020-0884-y.
19. C E Shannon. A Mathematical Theory of Communication. *Bell System Technical Journal*, 27(3):379–423, 1948. doi: 10.1002/j.1538-7305.1948.tb01338.x.
20. Giovanni B Brandani, Marieke Schor, Cait E MacPhee, Helmut Grubmüller, Ulrich Zachariae, and Davide Marenduzzo. Quantifying disorder through conditional entropy: an application to fluid mixing. *PloS one*, 8(6):e65617, 2013.
21. W. McGill. Multivariate information transmission. *Transactions of the IRE Professional Group on Information Theory*, 4(4):93–111, 1954.
22. Anthony J Bell. The co-information lattice. In *Proceedings of the Fifth International Workshop on Independent Component Analysis and Blind Signal Separation: ICA*, volume 2003. Citeseer, 2003.
23. Michael V LeVine and Harel Weinstein. NbIT - A New Information Theory-Based Analysis of Allosteric Mechanisms Reveals Residues that Underlie Function in the Leucine Transporter LeuT. *PLOS Computational Biology*, 10(5):1–15, 2014. doi: 10.1371/journal.pcbi.1003603.
24. A Ghassami and N Kiyavash. Interaction information for causal inference: The case of directed triangle. In *2017 IEEE International Symposium on Information Theory (ISIT)*, pages 1326–1330, 2017. ISBN 2157-8117 VO -. doi: 10.1109/ISIT.2017.8006744.
25. Abhijeet Kapoor, Gerard Martinez-Rosell, Davide Provasi, Gianni de Fabritiis, and Marta Filizola. Dynamic and Kinetic Elements of μ-Opioid Receptor Functional Selectivity. *Scientific Reports*, 7(1):11255, 2017. ISSN 2045-2322. doi: 10.1038/s41598-017-11483-8.
26. Aysima Hacisuleyman and Burak Erman. Entropy Transfer between Residue Pairs and Allostery in Proteins: Quantifying Allosteric Communication in Ubiquitin. *PLOS Computational Biology*, 13(1):1–23, 2017. doi: 10.1371/journal.pcbi.1005319.
27. Yinglong Miao, Alisha D Caliman, and J Andrew McCammon. Allosteric effects of sodium ion binding on activation of the m3 muscarinic g-protein-coupled receptor. *Biophysical journal*, 108(7):1796–1806, apr 2015. ISSN 1542-0086. doi: 10.1016/j.bpj.2015.03.003.
28. Kate L. White, Matthew T. Eddy, Zhan Guo Gao, Gye Won Han, Tiffany Lian, Alexander Deary, Nilkanth Patel, Kenneth A. Jacobson, Vsevolod Katritch, and Raymond C. Stevens. Structural Connection between Activation Microswitch and Allosteric Sodium Site in GPCR Signaling. *Structure*, 26(2):259–269.e5, 2018. ISSN 18784186. doi: 10.1016/j.str.2017.12.013.
29. Daria N Shalaeva, Dmitry A Cherepanov, Michael Y Galperin, Gert Vriend, and Armen Y Mulkidjanian. G protein-coupled receptors of class A harness the energy of membrane potential to increase their sensitivity and selectivity. *Biochimica et Biophysica Acta (BBA) - Biomembranes*, 1861(12):183051, 2019. ISSN 0005-2736. doi: https://doi.org/10.1016/j.bbamem.2019.183051.
30. Anirudh Ranganathan, Ron O Dror, and Jens Carlsson. Insights into the Role of Asp792.50 in $\beta 2$ Adrenergic Receptor Activation from Molecular Dynamics Simulations. *Biochemistry*, 53(46):7283–7296, nov 2014. ISSN 0006-2960. doi: 10.1021/bi5008723.
31. Vsevolod Katritch, Gustavo Fenalti, Enrique E Abola, Bryan L Roth, Vadim Cherezov, and Raymond C Stevens. Allosteric sodium in class A GPCR signaling. *Trends in Biochemical Sciences*, 39(5):233–244, 2014. ISSN 0968-0004. doi: https://doi.org/10.1016/j.tibs.2014.03.002.
32. Oliver F Lange and Helmut Grubmüller. Generalized correlation for biomolecular dynamics. *Proteins: Structure, Function, and Bioinformatics*, 62(4):1053–1061, 2006. doi: 10.1002/prot.20784.
33. Jendrik Schöppe, Janosch Ehrenmann, Christoph Klenk, Prakash Rucktooa, Marco Schütz, Andrew S Doré, and Andreas Plückthun. Crystal structures of the human neurokinin 1 receptor in complex with clinically used antagonists. *Nature communications*, 10(1):1–11, 2019.
34. Naomi R Latorraca, A J Venkatakrishnan, and Ron O Dror. GPCR Dynamics: Structures in Motion. *Chemical Reviews*, 117(1):139–155, jan 2017. ISSN 0009-2665. doi: 10.1021/acs.chemrev.6b00177.
35. A A Hagberg, D A Schult, and P J Swart. Exploring network structure, dynamics, and function using NetworkX. In *7th Python in Science Conference (SciPy 2008)*, 2008.
36. Vignir Isberg, Stefan Mordalski, Christian Munk, Krzysztof Rataj, Kasper Harpsøe, Alexander S. Hauser, Bas Vroling, Andrzej J. Bojarski, Gert Vriend, and David E. Gloriam. GPCRdb: An information system for G protein-coupled receptors. *Nucleic Acids Research*, 44(D1):D356–64, 2016. ISSN 13624962. doi: 10.1093/nar/gkv1178.
37. Benjamin Webb and Andrej Sali. Comparative Protein Structure Modeling Using MODELLER. *Current Protocols in Bioinformatics*, 54(1):5.6.1–5.6.37, 2016. doi: 10.1002/cpbi.3.
38. Gáspár Pándy-Szekeres, Christian Munk, Tsonko M Tsonkov, Stefan Mordalski, Kasper Harpsøe, Alexander S Hauser, Andrzej J Bojarski, and David E Gloriam. GPCRdb in 2018: adding GPCR structure models and ligands. *Nucleic Acids Research*, 46(D1):D440–D446, nov 2017. ISSN 0305-1048. doi: 10.1093/nar/gkx1109.
39. Warren L DeLano. Pymol: An open-source molecular graphics tool. *CCP4 Newsletter on protein crystallography*, 40(1):82–92, 2002.
40. Mark James Abraham, Teemu Murtola, Roland Schulz, Szilárd Páll, Jeremy C Smith, Berk Hess, and Erik Lindahl. GROMACS: High performance molecular simulations through multi-level parallelism from laptops to supercomputers. *SoftwareX*, 1-2:19–25, 2015. ISSN 2352-7110. doi: https://doi.org/10.1016/j.softx.2015.06.001.
41. Alan W Sousa da Silva and Wim F Vranken. ACPYPE - AnteChamber PYthon Parser interfacE. *BMC Research Notes*, 5(1):367, 2012. ISSN 1756-0500. doi: 10.1186/1756-0500-5-367.
42. Kresten Lindorff-Larsen, Stefano Piana, Kim Palmo, Paul Maragakis, John L Klepeis, Ron O Dror, and David E Shaw. Improved side-chain torsion potentials for the Amber ff99SB protein force field. *Proteins*, 78(8):1950–1958, jun 2010. ISSN 1097-0134. doi: 10.1002/prot.22711.
43. Joakim P M Jämbeck and Alexander P Lyubartsev. An Extension and Further Validation of an All-Atomistic Force Field for Biological Membranes. *Journal of Chemical Theory and Computation*, 8(8):2938–2948, aug 2012. ISSN 1549-9618. doi: 10.1021/ct300342n.
44. Christian Kandt, Walter L Ash, and D Peter Tieleman. Setting up and running molecular dynamics simulations of membrane proteins. *Methods*, 41(4):475–488, 2007. ISSN 1046-2023. doi: https://doi.org/10.1016/j.ymeth.2006.08.006.
45. William L Jorgensen, Jayaraman Chandrasekhar, Jeffry D Madura, Roger W Impey, and Michael L Klein. Comparison of simple potential functions for simulating liquid water. *The Journal of Chemical Physics*, 79(2):926–935, 1983. doi: 10.1063/1.445869.
46. Giovanni Bussi, Tatyana Zykova-Timan, and Michele Parrinello. Isothermal-isobaric molecular dynamics using stochastic velocity rescaling. *The Journal of Chemical Physics*, 130(7):74101, feb 2009. ISSN 0021-9606. doi: 10.1063/1.3073889.
47. Owen N. Vickery, Jan-Philipp Machtens, Giulia Tamburrino, Daniel Seeliger, and Ulrich Zachariae. Structural Mechanisms of Voltage Sensing in G Protein-Coupled Receptors. *Structure*, 24(6):997–1007, jun 2016. ISSN 0969-2126. doi: 10.1016/j.str.2016.04.007.
48. Owen N Vickery, Jan-Philipp Machtens, and Ulrich Zachariae. Membrane potentials regulating gpcrs: insights from experiments and molecular dynamics simulations. *Current Opinion in Pharmacology*, 30:44–50, 2016.
49. Berk Hess, Henk Bekker, Herman JC Berendsen, and Johannes GEM Fraaije. Lincs: a linear constraint solver for molecular simulations. *Journal of computational chemistry*, 18 (12):1463–1472, 1997.
50. Shuichi Miyamoto and Peter A Kollman. Settle: An analytical version of the shake and rattle algorithm for rigid water models. *Journal of computational chemistry*, 13(8):952–962, 1992.
51. Yoonji Lee, Songmi Kim, Sun Choi, and Changbong Hyeon. Ultraslow Water-Mediated Transmembrane Interactions Regulate the Activation of A2A Adenosine Receptor. *Biophysical journal*, 111(6):1180–1191, sep 2016. ISSN 1542-0086. doi: 10.1016/j.bpj.2016.08.002.
52. Naveen Michaud-Agrawal, Elizabeth J Denning, Thomas B Woolf, and Oliver Beckstein. MDAnalysis: A toolkit for the analysis of molecular dynamics simulations. *Journal of Computational Chemistry*, 32(10):2319–2327, jul 2011. ISSN 0192-8651. doi: 10.1002/jcc.21787.